

STOCHASTIC 3D MODELING OF AMORPHOUS MICROSTRUCTURES - A POWERFUL TOOL FOR VIRTUAL MATERIALS TESTING

Matthias Neumann¹, Volker Schmidt¹

¹Institute of Stochastics, Ulm University,
D-89069 Ulm, Germany
e-mail: matthias.neumann@uni-ulm.de, volker.schmidt@uni-ulm.de

Keywords: Virtual materials testing, Stochastic 3D modeling, Microstructure, Li-ion batteries, Solid oxide fuel cells, Effective conductivity.

Abstract. *We are going to introduce the concept of stochastic 3D modeling of geometrically complex (disordered) microstructures as a tool for virtual materials testing, including applications to battery electrodes as well as to electrodes of fuel cells, and solar cells. Using stochastic 3D models, one can generate a large variety of stochastically simulated microstructures with little computational effort. These virtual microstructures can be used as data basis to elucidate microstructure-property relationships. In this way, for example, effective conductivity can be expressed by microstructural characteristics such as volume fraction, tortuosity (windedness of transport paths) and constrictivity (bottleneck criterion) of the considered material phase. In another recent simulation study, we analysed more than 8000 virtual microstructures for various microstructural scenarios. Using data mining techniques like artificial neural networks and random forests, we were able to accurately predict effective conductivities given microstructure properties like volume fraction, tortuosity and constrictivity.*

1 INTRODUCTION

In many applications the functionality of materials strongly depends on their - mostly amorphous - microstructure. This is the case for, e.g. anodes in lithium-ion (Li-ion) batteries, which are a key technology for electric vehicles. The microstructure of these electrodes, consisting mainly of graphite particles and pores, strongly influences both, the transport of ions and electrons as well as degradation processes within the electrode, which are in turn important for the performance and lifetime of the battery. For microstructure effects in Li-ion batteries, see e.g. [1] and the references therein. Porous microstructures appear also in electrodes of solid oxide fuel cells (SOFC), a technology for electricity generation, which is more efficient, more reliable and has less environmental impact compared to conventional energy generation. Like in Li-ion batteries the porous microstructures in SOFC are of high relevance for the performance of these fuel cells as well as for their degradation processes. See e.g. [2] for the microstructure influence in SOFC electrodes where the solid phase consists of nickel (Ni) and yttria-stabilized zirconia (YSZ).

Due to this microstructural influence on the functionality of Li-ion batteries and SOFC, two issues have to be clarified in order to improve the functionality of these materials. At first, it is important to understand how the microstructure of the electrode is quantitatively related to the corresponding effective properties. The second issue is how the production parameters of the electrodes influence the microstructure.

The progress in tomographic 3D imaging during the last decades has enabled detailed microstructure analysis, see [3] for a methodological overview. For microstructure analysis in the context of Li-ion batteries and SOFC we refer, e.g., to [4] and [5]. By the aid of numerical modeling it is possible to simulate the corresponding effective properties, like effective conductivity. Although this combination of image analysis and numerical simulation allows a direct investigation of the relationship between well-defined microstructure characteristics and effective transport properties ([6] to [9]), it is strongly limited by the high costs of tomographic 3D imaging.

An alternative approach which combines image analysis and numerical simulations with stochastic 3D modeling of amorphous microstructures solves this problem. Tools from spatial statistics and stochastic geometry, see e.g. [10], are used to develop parametric stochastic 3D models for the generation of virtual but realistic microstructures on the basis of image data from real microstructures. Once developed, a stochastic 3D model can be used to approach both of the above mentioned issues. On the one hand, the parameters of the stochastic 3D model can be varied to obtain virtual microstructures within a wide range of microstructure characteristics. Then, numerical simulations can be applied to these virtual microstructures to simulate the corresponding effective properties, such that the quantitative relationship between microstructure characteristics and effective properties can be efficiently investigated, see e.g. [11] and [12]. On the other hand, in case that there is image data of microstructures available, where the microstructures are produced under different conditions (e.g. under different sinter temperatures like in [13]), the parameters of the stochastic 3D model might be fit to microstructures generated with different production parameters. An interpolation between model parameters and production parameters allows to predict virtual microstructures for production parameters where no 3D images are available. This was successfully done for solar cells produced with different spin coating velocities in [14]. Once the relationship between production parameters and microstructure is understood one can find optimal production parameters by numerical simulations of effective properties.

Summarizing the above, stochastic 3D modeling can be used for investigating the relationship between microstructure characteristics and effective properties as well as the relationship between microstructure characteristics and production parameters. Where we test the functionality of virtual microstructures by simulating their effective properties, the combination of mathematical image analysis, stochastic 3D modeling of amorphous microstructures, and numerical modeling of (spatially resolved) effective properties on complex geometries is, what we refer to as virtual materials testing.

In the present paper we give an overview of stochastic 3D modeling of amorphous microstructures, which is essential for virtual materials testing. The paper is organized as follows. Models for electrode materials in Li-ion batteries ([15], [16]), and for SOFC ([13], [17]) are reviewed in Sections 2 and 3, respectively. In Section 4 we present a method to derive empirical formulas that describe the quantitative relationship between microstructure characteristics and effective conductivity in porous microstructures ([11], [12]). Section 5 concludes the paper.

2 LITHIUM-ION BATTERIES

In [16] a stochastic 3D model for the anode microstructure of so-called energy cells in Li-ion batteries has been developed on the basis of experimental image data obtained by X-ray tomography, see Figure 1. The anode mainly consists of a connected network of graphite particles and pores between the particles.

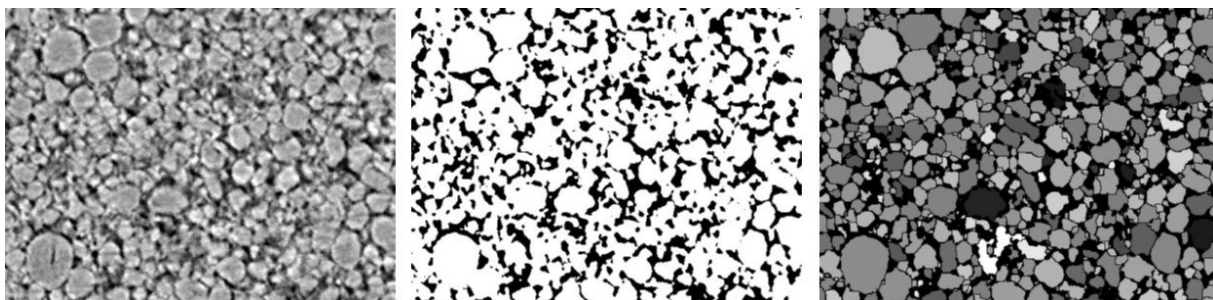


Figure 1: 2D slice of experimental image data: Grayscale image obtained by X-ray tomography (left) has been binarized (center). The application of the watershed transform has led to an extraction of single particles (right).²

2.1 Stochastic modeling of particle shapes

Since the shape of graphite particles observed in data is neither spherical nor ellipsoidal, the single particles in the considered anode material have been modeled by the so-called spherical harmonics expansion, see [15] and [18]. This approach is based on the fact that any (star-shaped) particle in 3D is completely determined by its barycenter and a function $r : [0, \pi] \times [0, 2\pi) \rightarrow [0, \infty)$, where $r(\theta, \phi)$ denotes the elongation of the particle in direction $(\sin \theta \cos \phi, \sin \theta \sin \phi, \cos \theta)$. By the aid of the so-called spherical harmonics functions $\{Y_l^m : [0, \pi] \times [0, 2\pi) \rightarrow [0, \infty) : l, m \geq 0\}$, the radius function r can be represented as

$$r(\theta, \phi) = \sum_{l=0}^{\infty} \sum_{m=-l}^l c_l^m Y_l^m(\theta, \phi) \approx \sum_{l=0}^L \sum_{m=-l}^l c_l^m Y_l^m(\theta, \phi) \quad (1)$$

²Reprinted from [16], Figure 1, with permission from Elsevier.

for $L \geq 1$ large enough and spherical harmonics coefficients $c_l^m \in \mathbb{R}$ with $0 \leq l$ and $-l \leq m \leq l$. For details and the definition of the spherical harmonics functions Y_l^m the reader is referred to [15].

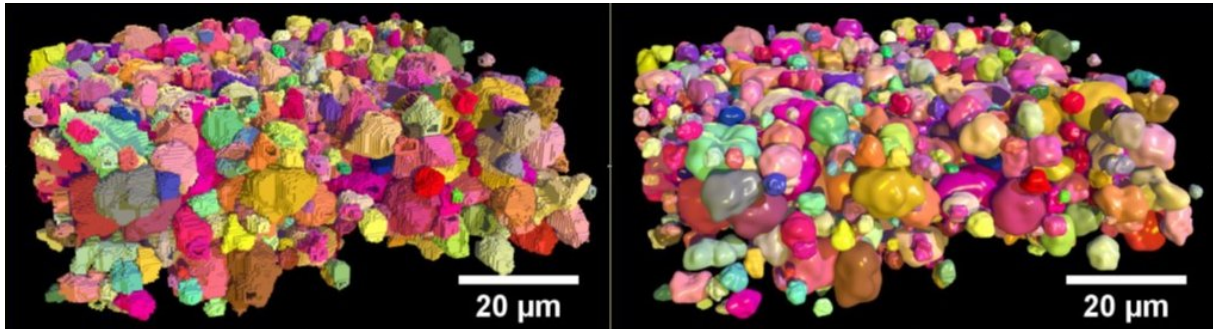


Figure 2: 3D voxel representation of graphite particles (left) and their spherical harmonics representation (right).³

Equation (1) implies that each (star-shaped) particle is completely determined by its spherical harmonics coefficients and, therefore, the particle can be approximated by a finite number of coefficients. In [15] a method for estimating L and the spherical harmonics coefficients $c_l^m \in \mathbb{R}$ with $0 \leq l \leq L$ and $-l \leq m \leq l$ from image data is described. This method has been successfully applied to experimental image data showing particles in battery anodes, see Figure 2. The single particles have been extracted from grayscale images with well-known methods from image analysis, to be more precise the watershed transform, see e.g. [19], has been used after binarization of the grayscale images, see Figure 1.

Since the shape of each graphite particle is appropriately described by a finite number of real-valued coefficients, the spherical harmonics representation leads to an enormous compression of information contained in the original (grayscale) image data.

2.2 Stochastic modeling of anode microstructure

In total, a parametric representation of image data is obtained by the method proposed in [15]. The anode material is completely described by the barycenters of particles and their spherical harmonics coefficients. In [16] statistical analysis of this parametric representation is the basis for stochastic 3D modeling of anode microstructures in Li-ion batteries.

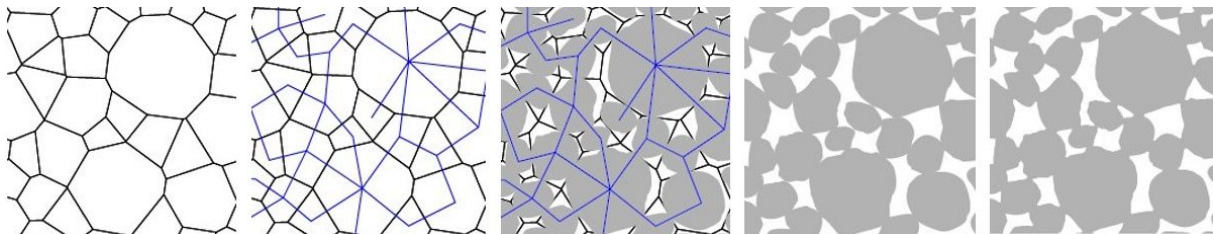


Figure 3: 2D sketch of the modeling idea: Random tessellation model determines the locations of particles (1). Connections between particles have been modeled by a random graph (2). Particle shapes have been modeled using spherical harmonics (3). Connected particle system before (4) and after morphological closing (5).⁴

³Reprinted from [15], Figure 11, with permission from Elsevier.

The model idea, sketched in Figure 3, is the following. At first the locations, at which the single particles are placed, have been modeled by a random Laguerre tessellation, see [20]. That is to say that the 3D space is partitioned into polytopes, the size distribution of which can be controlled by model parameters. In a second step, connections between single particles have been modeled by a completely connected random graph, i.e., edges are put between neighboring polytopes according to a certain probabilistic rule. Within each polytope a particle is placed using spherical harmonics, such that particles overlap if they are connected by an edge in the random graph. This graph model ensures that the modeled particle system is completely connected. Finally, morphological closing is applied to the particle system in order to smooth the sharp edges at the contacts between particles. Note that the volume fraction of the particle system can be adjusted by model parameters, which have been fitted to experimental image data.

Besides a visual comparison between virtual microstructures generated by the fitted model and experimental image data, see Figure 4, an extensive quantitative validation regarding certain microstructure characteristics has been performed and discussed in [16]. Exemplarily, the spherical contact distribution functions [10] of the particle phase, which are nearly identical for virtual and experimental microstructures, are shown in Figure 4.

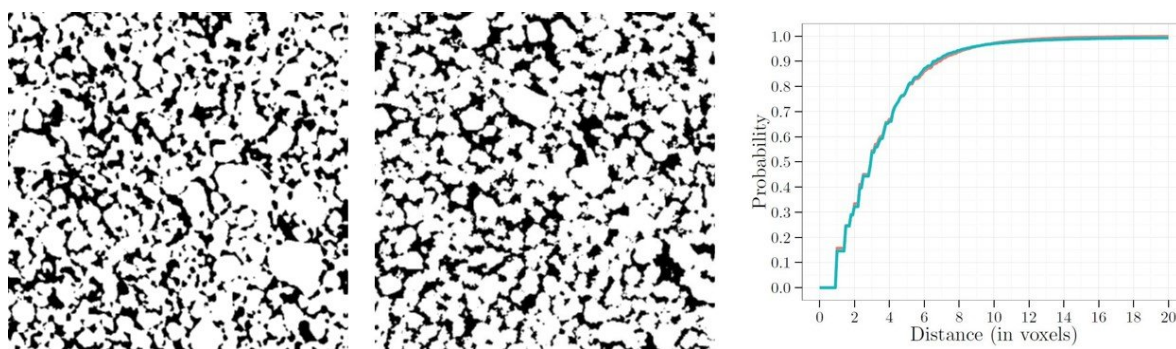


Figure 4: 2D slice of experimental image data from anode material (left) compared to a 2D slice of a virtual 3D microstructure generated by the stochastic model (center). Spherical contact distribution functions computed for experimental (red) and simulated (blue) microstructures are nearly identical.⁵

Thus, in [15] and [16] flexible modeling techniques have been developed for 3D microstructures in Li-ion batteries. In particular, a stochastic 3D model has been established which is able to generate virtual microstructures that are statistically similar to experimental microstructures. In a forthcoming paper, the model is further validated by numerical 3D electrochemical simulations, which are applied to experimental and virtual anodes [21]. Additionally, extensions of the stochastic microstructure model, which overcome small differences in electrochemical behaviour, are proposed. The model will be used for investigating the relationship between microstructure characteristics and the functionality of Li-ion batteries, i.e. for virtual materials testing.

3 SOLID OXIDE FUEL CELLS

In this section we summarize the modeling approaches proposed in [13] and [17]. While in [13] a stochastic microstructure model has been fitted to three cathode materials produced

⁴Reprinted from [16], Figure 2, with permission from Elsevier.

⁵Reprinted from [16], Figures 10 and 11, with permission from Elsevier.

with different sinter temperatures, the model in [17] is able to generate virtual, but realistic three-phase microstructures, where all three phases are completely connected.

3.1 Stochastic 3D modeling of $\text{La}_{0.6}\text{Sr}_{0.4}\text{CoO}_{3-\delta}$ cathodes

The considered $\text{La}_{0.6}\text{Sr}_{0.4}\text{CoO}_{3-\delta}$ (LSC) cathodes consist of sintered spherical LSC particles, which form a connected particle system, and pores, see Figure 6. Thus the microstructure has been modeled by a completely connected union of slightly overlapping spheres. To begin with, a structural segmentation of the binarized image data, obtained by FIB-SEM tomography, has been performed to represent the LSC phase by a union of overlapping spheres. For this purpose, tools from image analysis like the watershed algorithm [19] and the Hough transform [22] are used.

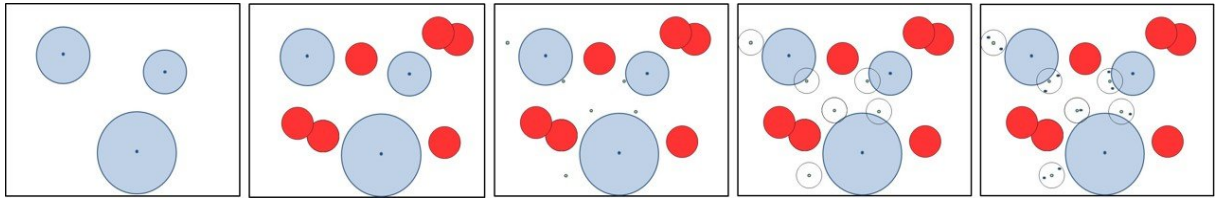


Figure 5: Modeling idea for the midpoints of the sphere system sketched in 2D: Non-overlapping large spheres are randomly distributed (1), where pore former (red circles) is modeled in the remaining space (2). Cluster centers of small spheres (3) determine regions (4) in which the midpoints of small spheres are distributed (5).

Like in the case of battery anodes considered in Section 2, this kind of structural segmentation can be understood as a compression of image data, since the microstructure has been appropriately represented by the midpoints and radii of the spheres. In a second step a model for random sphere systems, a so-called germ-grain model [10], is developed which generates sphere systems that are similar to those extracted from image data.

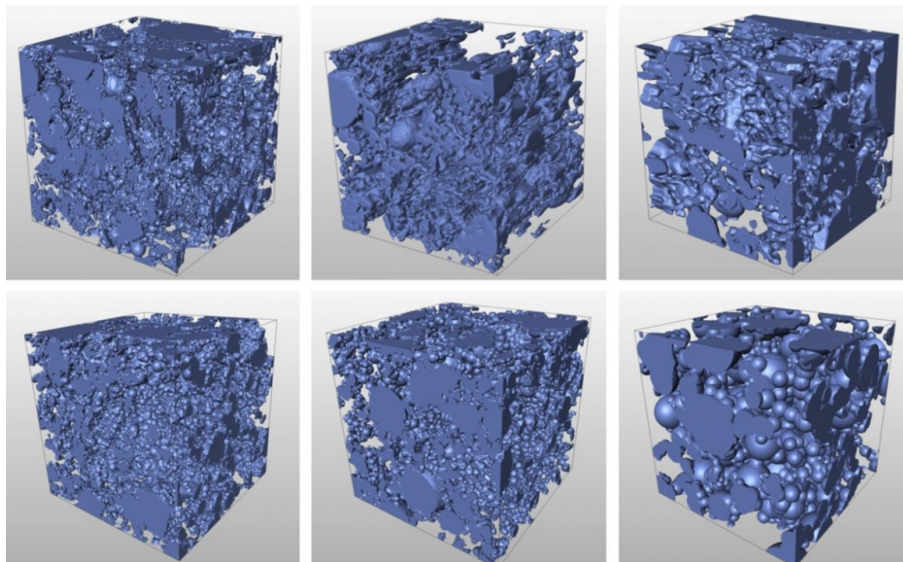


Figure 6: 3D images of real (top) and virtual microstructures (bottom). The structures correspond to different sinter temperatures (from left to right: 750°C , 850°C , 950°C).⁶

The modeling of sphere midpoints takes into account that small particles are accumulated around large spheres and that large void regions occur due to pore former. The sphere midpoints have been modeled in three steps using random point processes, see e.g. [10]. At first large spheres are distributed completely at random under the condition that they do not overlap each other. Then, the void regions are determined according to a Boolean model [23] with spherical grains in the remaining space. Finally the midpoints of small spheres are clustered around the large spheres, see Figure 5. The radii of the small spheres are determined such that volume fraction and connectivity properties of the sphere systems extracted from experimental image data are statistically matched. Similar as in [16] a graph model is used for this purpose. For further details we refer to [13].

The model has been fitted to three cathodes, produced with three different sinter temperatures of 750°C, 850°C and 950°C. Figure 6 shows a good visual accordance between image data and virtual structures generated by the model. Furthermore, in [13] a quantitative comparison of microstructure characteristics is performed and, in combination with numerical modeling, the influence of different sinter temperatures on the electrode performance can be investigated. The achieved goodness-of-fit shows a high flexibility of the model since all three microstructures produced with different sinter temperatures can be described by one and the same model type, although their microstructure characteristics differ strongly from each other.

3.2 Stochastic 3D modeling of three-phase Ni-YSZ anodes

In Sections 2.2 and 3.1 the material to be modeled consists of pores and mainly one single (homogeneous) solid phase. In this section a model for three-phase microstructures with two different solid (sub-) phases is described, which has been introduced in [17]. The model exhibits the desirable property that it reproduces microstructures where all three phases are completely connected. Three-phase microstructure modeling is important since not only the geometry of single phases influences the functionality of Ni-YSZ anodes, but also the length and the geometry of the triple phase boundary (TPB), at which chemical reactions take place.

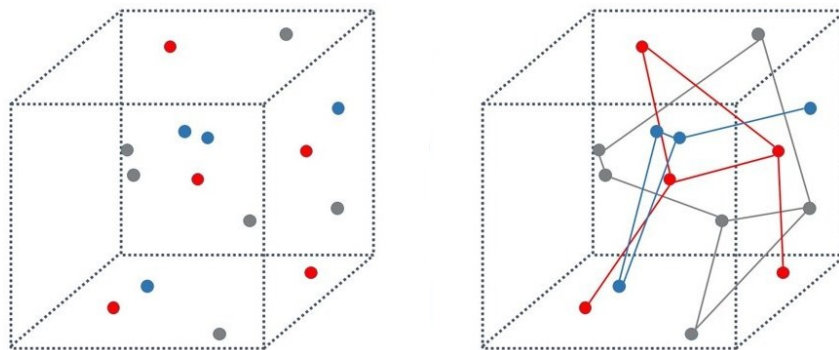


Figure 7: Modeling idea: Three random point patterns (consisting of blue, gray and red points, respectively) are distributed completely at random in the three-dimensional space (left). On each of these point patterns a geometric graph is modeled (right).

A parametric random graph in the three-dimensional space has been modeled for each phase, the vertices of which are distributed completely at random, see Figure 7. These graphs build the backbones of the three phases, which are Voronoi tessellations with respect to the edge set

⁶Reprinted from [13], Figure 15, with permission from Elsevier.

of the three graphs, i.e. each point $x \in \mathbb{R}^3$ is allocated to the phase the corresponding graph of which is closer to x than the other two graphs.

By this approach the model is able to mimic connectivity properties of experimental image data gained by FIB-tomography. It is even possible to simulate virtual microstructures with arbitrary volume fractions and completely connected phases. A slight generalization of the model has enabled a good fit to the experimental image data recently discussed in [24], see Figure 8.

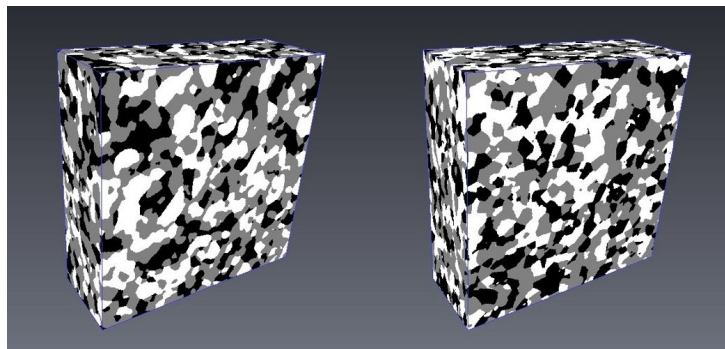


Figure 8: Image data of real (left) and virtual (right) Ni-YSZ anodes.

Simulations of the effective conductivity σ_{eff} for image data of real and virtual Ni-YSZ anodes by means of the finite element method (FEM) has shown that the model is close to the real microstructures with respect to effective properties. Besides the development of new techniques for stochastic 3D modeling of three-phase microstructures, the model proposed in [17] is the basis of virtual materials testing for Ni-YSZ anodes. In a further work the area specific resistance (ASR) of virtual Ni-YSZ microstructures with systematically varied microstructure characteristics is simulated by a FE model for the anode reaction mechanism that takes into account the specific microstructure characteristics, in particular the length of TPB. Performing this kind of virtual materials testing we expect new insights about the microstructure influence on the ASR.

4 VIRTUAL MATERIALS TESTING

In the previous sections stochastic 3D models have been presented, which are fitted to image data of real microstructures in order to study the microstructure of various energy materials. Moreover, it is of general interest to investigate quantitative relationships between microstructure characteristics and effective properties. In this section we focus on the so-called M -factor, a normed measure for the microstructure influence on effective conductivity. It is defined by

$$M = \frac{\sigma_{\text{eff}}}{\sigma_0}, \quad (2)$$

where σ_0 denotes the intrinsic conductivity of the material. Virtual materials testing contributes to find an expression of the M -factor in terms of microstructure characteristics ([11], [12]).

Leaned on [25] the investigations in [11] and [12] assumed that volume fraction ε , tortuosity τ measuring the length of (shortest) transport paths and a constriction factor β measuring the strength of bottleneck effects are the most important characteristics for effective conductivity in porous microstructures. For tortuosity, two different approaches, i.e., mean geometric and

mean geodesic tortuosity denoted by τ_{geom} and τ_{geod} have been taken into account [12]. The definition of β is based on the concept of continuous phase size distribution and a geometric simulation of mercury intrusion porosimetry [26].

The idea was to develop a stochastic 3D model which is flexible regarding the microstructure characteristics ε , τ_{geom} , τ_{geod} and β . Then, σ_{eff} , and thus the M -factor, of virtual microstructures with different constellations for ε , τ_{geom} , τ_{geod} and β can be simulated by FEM. The generated database has enabled an efficient investigation of the quantitative microstructure influence on the M -factor.

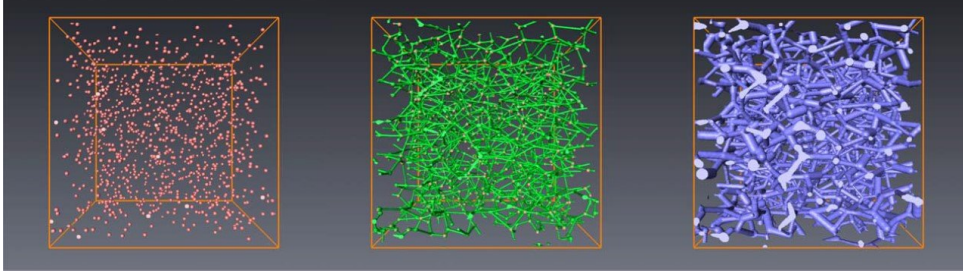


Figure 9: Modeling idea: Vertices are distributed completely at random (left), before edges are put (center). Random dilation of edges leads to virtual microstructures (right).⁷

The stochastic 3D model is based on an anisotropic random graph model, where the anisotropy can be controlled by model parameters. The vertices of the graph are distributed completely at random in the three-dimensional space. The edges of the graph are randomly diluted, where the variance of the dilation radii influences the constrictivity of the microstructure strongly. Note that the model graph is completely connected which ensures complete connectivity of the conducting phase. The modeling idea is visualized in Figure 9.

By means of the stochastic 3D model 49 virtual microstructures for a wide range of ε , τ_{geom} , τ_{geod} and β have been generated and the corresponding effective conductivities are simulated by FEM. Using error-minimization the relationship

$$M = \min \left\{ 1, 2.03 \frac{\varepsilon^{1.57} \beta^{0.72}}{\tau_{\text{geom}}^2} \right\} \quad (3)$$

has been established in [11] and further refined in [12] using the concept of geodesic tortuosity instead of geometric tortuosity. This has led to

$$M = \frac{\varepsilon^{1.15} \beta^{0.37}}{\tau_{\text{geod}}^{4.39}}. \quad (4)$$

Both relationships fit better to the virtual microstructures than the existing ones from literature. Furthermore, validation with experimental image data has been performed in [12], which shows that Equation (4) derived by virtual materials testing is able to predict the M -factor of real microstructures quite well by the microstructure characteristics ε , τ_{geod} and β .

A forthcoming paper [27] is under preparation in which an extensive simulation study with around 8000 virtual microstructures is performed. In this work methods from statistical learning [28] are combined with virtual materials testing for further improvement of quantitative relationships between microstructure characteristics and the M -factor.

⁷Reprinted from [11], Figure 3, with permission from J. Wiley & Sons.

5 CONCLUSION

In the present survey paper the concept of virtual materials testing is presented. It is a method, which combines mathematical image analysis, stochastic 3D modeling of amorphous microstructures, and numerical modeling of (spatially resolved) effective properties on complex geometries for an efficient investigation of the relationship between microstructure characteristics of functional materials and their effective properties.

The focus of the present paper is on stochastic 3D modeling of microstructures in Li-ion batteries and SOFC. In Section 4 it is described how quantitative relationships between the microstructure characteristics volume fraction, tortuosity, constrictivity on the one hand and effective conductivity on the other hand can be established. Virtual materials testing is neither restricted to Li-ion batteries and SOFC nor to effective conductivity. Virtual materials testing opens the possibility to investigate amorphous structures of various further materials, e.g., in polymers solar cells [12] or aluminium alloys [29] as well as various further effective properties like e.g. exciton quenching efficiency [14] or mechanical stress-strain curves [30].

REFERENCES

- [1] J. R. Wilson, J. S. Cronin, S. A. Barnett, S. J. Harris. Measurement of three-dimensional microstructure in a LiCoO_2 positive electrode. *Journal of Power Sources*, **196**, 3443–3447, 2011.
- [2] B. S. Prakash, S. S. Kumar, S. T. Aruna. Properties and development of Ni/YSZ as an anode material in solid oxide fuel cell: A review. *Renewable and Sustainable Energy Reviews*, **36**, 149–179, 2014.
- [3] S. Torquato. *Random Heterogeneous Materials: Microstructure and Macroscopic Properties*. Springer, New York, 2013.
- [4] P. R. Shearing, L. E. Howard, P. S. Jørgensen, N. P. Brandon, S. J. Harris. Characterization of the 3-dimensional microstructure of a graphite negative electrode from a Li-ion battery. *Electrochemistry Communications*, **12**, 374–377, 2010.
- [5] J. R. Wilson, W. Kobsiriphat, R. Mendoza, H.-Y. Chen, J. M. Hiller, D. J. Miller, K. Thornton, P. W. Voorhees, S. B. Adler, S. A. Barnett. Three-dimensional reconstruction of a solid-oxide fuel-cell anode. *Nature Materials*, **5**, 541–544, 2006.
- [6] M. Doyle, T. F. Fuller, J. Newman. Modeling of galvanostatic charge and discharge of the lithium/polymer/insertion cell. *Journal of the Electrochemical Society*, **140**, 1526–1533, 1993.
- [7] L. Holzer, B. Iwanschitz, T. Hocker, L. Keller, O. M. Pecho, G. Sartoris, P. Gasser, B. Muench. Redox cycling of Ni-YSZ anodes for solid oxide fuel cells: Influence of tortuosity, constriction and percolation factors on the effective transport properties. *Journal of Power Sources*, **242**, 179–194, 2013.
- [8] N. Shikazono, D. Kanno, K. Matsuzaki, H. Teshima, S. Sumino, N. Kasagi. Numerical assessment of SOFC anode polarization based on three-dimensional model microstructure reconstructed from FIB-SEM images. *Journal of the Electrochemical Society*, **157**, B665–B672, 2010.

- [9] S. Tippmann, D. Walper, L. Balboa, B. Spier, W. G. Bessler. Low-temperature charging of lithium-ion cells part I: Electrochemical modeling and experimental investigation of degradation behavior. *Journal of Power Sources*, **252**, 305–316, 2014.
- [10] S. N. Chiu, D. Stoyan, W. S. Kendall, J. Mecke. *Stochastic Geometry and its Applications*. J. Wiley & Sons, Chichester, 3rd edition, 2013.
- [11] G. Gaiselmann, M. Neumann, O. M. Pecho, T. Hocker, V. Schmidt, L. Holzer. Quantitative relationships between microstructure and effective transport properties based on virtual materials testing. *AIChE Journal*, **60**, 1983–1999, 2014.
- [12] O. Stenzel, O. M. Pecho, M. Neumann, V. Schmidt, L. Holzer. Predicting effective conductivities based on geometric microstructure characteristics. *AIChE Journal*, *in print*, 2016.
- [13] G. Gaiselmann, M. Neumann, L. Holzer, T. Hocker, M. Prestat, V. Schmidt. Stochastic 3D modeling of $\text{La}_{0.6}\text{Sr}_{0.4}\text{CoO}_{3-\delta}$ cathodes based on structural segmentation of FIB-SEM images. *Computational Materials Science*, **67**, 48–62, 2013.
- [14] O. Stenzel, L. Koster, R. Thiedmann, S. D. Oosterhout, R. A. J. Janssen, V. Schmidt. A new approach to model-based simulation of disordered polymer blend solar cells. *Advanced Functional Materials*, **22**, 1236–1244, 2012.
- [15] J. Feinauer, A. Spetl, I. Manke, S. Strege, A. Kwade, A. Pott, V. Schmidt. Structural characterization of particle systems using spherical harmonics. *Materials Characterization*, **106**, 123–133, 2015.
- [16] J. Feinauer, T. Brereton, A. Spetl, M. Weber, I. Manke, V. Schmidt. Stochastic 3D modeling of the microstructure of lithium-ion battery anodes via gaussian random fields on the sphere. *Computational Materials Science*, **109**, 137–146, 2015.
- [17] M. Neumann, J. Staněk, O. M. Pecho, L. Holzer, V. Beneš, V. Schmidt. Stochastic 3D modeling of complex three-phase microstructures in SOFC-electrodes with completely connected phases. *Computational Materials Science*, *under revision*, 2016.
- [18] E. J. Garboczi. Three-dimensional mathematical analysis of particle shape using X-ray tomography and spherical harmonics: Application to aggregates used in concrete. *Cement and Concrete Research*, **32**, 1621–1638, 2002.
- [19] J. B. T. M. Roerdink, A. Meijster. The watershed transform: Definitions, algorithms and parallelization strategies. *Fundamenta informaticae*, **41**, 187–228, 2000.
- [20] C. Lautensack, S. Zuyev. Random Laguerre tessellations. *Advances in applied probability*, **40**, 630–650, 2008.
- [21] S. Hein, J. Feinauer, D. Westhoff, I. Manke, V. Schmidt, A. Latz. 3D electrochemical simulations of experimental and virtual anodes in lithium-ion batteries. *Working paper*, 2016.
- [22] B. Jähne. *Digital Image Processing*. Springer, Berlin, 2005.

- [23] I. Molchanov. *Statistics of the Boolean Model for Practitioners and Mathematicians*. J. Wiley & Sons, Chichester, 1997.
- [24] O. M. Pecho, O. Stenzel, P. Gasser, M. Neumann, V. Schmidt, T. Hocker, R. J. Flatt, L. Holzer. 3D microstructure effects in Ni-YSZ anodes: Prediction of effective transport properties and optimization of redox-stability. *Materials*, **8**, 5554–5585, 2015.
- [25] J. Van Brakel, P. M. Heertjes. Analysis of diffusion in macroporous media in terms of a porosity, a tortuosity and a constrictivity factor. *International Journal of Heat and Mass Transfer*, **17**, 1093–1103, 1974.
- [26] L. Holzer, D. Wiedenmann, B. Münch, L. Keller, M. Prestat, P. Gasser, I. Robertson, B. Grobéty. The influence of constrictivity on the effective transport properties of porous layers in electrolysis and fuel cells. *Journal of Materials Science*, **48**, 2934–2952, 2013.
- [27] O. Stenzel, M. Neumann, O. M. Pecho, L. Holzer, V. Schmidt Big data for microstructure-property relationships: A case study of predicting effective conductivities. *Working paper*, 2016.
- [28] J. Friedman, T. Hastie, R. Tibshirani. *The Elements of Statistical Learning*. Springer, Berlin, 2001.
- [29] G. Gaiselmann, O. Stenzel, A. Kruglova, F. Muecklich, V. Schmidt. Competitive stochastic growth model for the 3D morphology of eutectic Si in Al–Si alloys. *Computational Materials Science*, **69**, 289–298, 2013.
- [30] M. Roland, A. Kruglova, G. Gaiselmann, T. Brereton, V. Schmidt, F. Mücklich, S. Diebels. Numerical simulation and comparison of a real Al–Si alloy with virtually generated alloys. *Archive of Applied Mechanics*, **85**, 1161–1171, 2015.